JB
Journals.ASM.org

Coordination of FocA and Pyruvate Formate-Lyase Synthesis in *Escherichia coli* Demonstrates Preferential Translocation of Formate over Other Mixed-Acid Fermentation Products

Lydia Beyer, Claudia Doberenz, Dörte Falke, Doreen Hunger, Bernhard Suppmann,* R. Gary Sawers

Institute for Biology/ Microbiology, Martin-Luther University Halle-Wittenberg, Halle (Saale), Germany

Enterobacteria such as *Escherichia coli* generate formate, lactate, acetate, and succinate as major acidic fermentation products. Accumulation of these products in the cytoplasm would lead to uncoupling of the membrane potential, and therefore they must be either metabolized rapidly or exported from the cell. *E. coli* has three membrane-localized formate dehydrogenases (FDHs) that oxidize formate. Two of these have their respective active sites facing the periplasm, and the other is in the cytoplasm. The bidirectional FocA channel translocates formate across the membrane delivering substrate to these FDHs. FocA synthesis is tightly coupled to synthesis of pyruvate formate-lyase (PflB), which generates formate. In this study, we analyze the consequences on the fermentation product spectrum of altering FocA levels, uncoupling FocA from PflB synthesis or blocking formate metabolism. Changing the *focA* translation initiation codon from GUG to AUG resulted in a 20-fold increase in FocA during fermentation and an ~3-fold increase in PflB. Nevertheless, the fermentation product spectrum throughout the growth phase remained similar to that of the wild type. Formate, acetate, and succinate were exported, but only formate was reimported by these cells. Lactate accumulated in the growth medium only in mutants lacking FocA, despite retaining active PflB, or when formate could not be metabolized intracellularly. Together, these results indicate that FocA has a strong preference for formate as a substrate *in vivo* and not other acidic fermentation products. The tight coupling between FocA and PflB synthesis ensures adequate substrate delivery to the appropriate FDH.

Formate is a signature fermentation product of many obligate and facultative anaerobes, particularly of the enterobacteria (1, 2). Due to its low redox potential (E^{o} −420 mV) formate is also an important electron donor and energy source for many microorganisms. With a pKa of 3.75, formate is mainly present as the monovalent anionic species at neutral pH, which means that it must be transported actively across the cytoplasmic membrane. Genetic studies performed with *Escherichia coli* originally demonstrated that the product of the *focA* (formate channel) gene has a key function in formate translocation during fermentative growth because mutants unable to synthesize FocA have defects in formate import as well as export (3, 4). Recent structural and biophysical studies have confirmed that FocA is a homopentameric channel, which shows structural similarity to the aquaporin family of membrane proteins (5–7). How bidirectional substrate translocation is controlled *in vivo*, however, is still unclear.

Although FocA is the archetype for this class of membrane proteins, phylogenetic studies have revealed that the FNT (formate-nitrite transporter) family is widely distributed among the archaea and bacteria and includes several thousand members (8), suggesting that this family is likely evolutionarily ancient. As well as a conserved pentameric structure, the FNT protein family has in common that members translocate small monovalent anionic species such as formate, nitrite, or hydrosulfide across bacterial cytoplasmic membranes (5–9). Intracellular accumulation of these substances can result in uncoupling of the membrane potential and thus these potentially toxic compounds must be either rapidly metabolized or exported from the cell. However, because formate and nitrite are also important electron and nitrogen donors, respectively, their controlled uptake is important for many microbes. FNT channels offer microbial cells the possibility of controlled uptake of these compounds when they are required and available, possibly coupled to proton import (4, 5, 10).

Identifying the features of the FNT proteins that govern their *in vivo* substrate specificity and "gating" (4, 10) is also an important goal of current research. A recent electrophysiological study performed on purified FocA isolated from *Salmonella enterica* serovar Typhimurium (10) has demonstrated that it is capable of translocating not only formate but acetate and lactate *in vitro*, leading to the suggestion that it might be an exporter of a number of the mixed-acid fermentation products in enterobacteria.

In *E. coli* the *focA* gene is cotranscribed with the gene encoding pyruvate formate-lyase (PflB), the glycyl radical enzyme responsible for formate production (4, 11, 12). Expression of the *focApflB* operon is induced by anaerobiosis, and this is controlled by the FNR and ArcA transcription factors (13, 14). Operon expression is induced under conditions resulting in pyruvate accumulation and, although IHF is required to mediate pyruvate-dependent induction (15), the mechanism underlying this control is still unclear. Transcription of the operon is also complex, involving multiple promoters, as well as transcript processing events (16, 17). The consequence of this elaborate regulation is that the cell is able to maintain tight coordination of FocA and PflB levels. This

Received 26 November 2012 **Accepted** 10 January 2013
Published ahead of print 18 January 2013
Address correspondence to R. Gary Sawers, gary.sawers@mikrobiologie.uni-halle.de.
* Present address: Bernhard Suppmann, Roche Diagnostics GmbH, Penzberg, Germany.

doi:10.1128/JB.02166-12

TABLE 1 Strains used in this study

Strain	Genotype[a]	Source or reference
MC4100	F$^-$ *araD139* Δ(*argF-lac*)*U169 ptsF25 deoC1 relA1 flbB5301 rspL150*	19
FM460	Like MC4100 but Δ*selC400*::Kan^r	20
RM201	Like MC4100 but Δ*pfl-25*Ω (pfl::cat pACYC184)	11
RM220	Like MC4100 but Δ*pflB-pflA*	21
REK700	Like MC4100 but *focA* (GUG codon of *focA* converted to UUU)	4
REK701	Like MC4100 but *focA* (*focA* codons 114 and 115 changed to UAG and UAA, respectively)	4
REK702	Like MC4100 but *focA* (GUG codon of *focA* converted to AUG)	4
REK703	Like MC4100 but *focA* (GUG codon of *focA* converted to GUC)	4
SEC702	Like REK702 but *selC400*::Kan^r	This study
SEC703	Like REK703 but *selC400*::Kan^r	This study
WL308	Like MC4100 but Δ(*fdhD-fdhE*)::MudI(Ap^r *lac*)	22

[a] Ap^r, ampicillin resistance; Kan^r, kanamycin resistance.

means that when formate levels increase due to the activity of PflB during mixed-acid fermentation sufficient FocA is available to export it across the cytoplasmic membrane, preventing potential toxicity and uncoupling effects (1, 18).

In the present study we addressed the effects of altering expression of the *focA-pflB* operon on formate levels in the growth medium. We also examined the consequences for the cell of decoupling *focA* and *pflB* expression and to what extent these changes influence the mixed-acid fermentation product spectrum. Our findings suggest that the tight coordination between FocA and PflB synthesis is important for efficient and specific delivery of formate to the formate dehydrogenases (FDHs), which are localized on either side of the cytoplasmic membrane.

MATERIALS AND METHODS

Strains and growth conditions. All bacterial strains used in the present study are listed in Table 1. Strains were grown in Luria broth or the buffered, rich medium TYEP (TYEP, 1% [wt/vol] tryptone, 0.5% [wt/vol] yeast extract, 100 mM potassium phosphate [pH 6.5]) as described previously (23). Supplements, when required, were added to the following final concentrations: 40 mM glucose and 75 or 200 mM sodium hypophosphite. M9 minimal medium (24) was used for the hypophosphite sensitivity assay, whereas Werkmann minimal medium (WM-medium [25]), composed of 50 mM disodium phosphate, 100 mM potassium dihydrogen phosphate, 15 mM ammonium sulfate, 1 mM magnesium sulfate, 0.1 mM calcium chloride, and 80 mM glucose (pH 6.5), was used for analysis of the fermentation products. Aerobic cultures were incubated on a rotary shaker (250 rpm) and at 37°C. Anaerobic growths were performed at 37°C in sealed bottles filled with anaerobic growth medium. When required, the growth medium was solidified with 1.5% (wt/vol) agar. All of the growth media were supplemented with 0.1% (vol/vol) SLA trace element solution (26). The antibiotics chloramphenicol, kanamycin, tetracycline, and ampicillin, when required, were added to the medium at final concentrations of 12.5, 50, 15, and 100 μg ml^{-1}, respectively.

Strain construction. The *selC400* allele was transduced from strain FM460 (20) into different *E. coli* genetic backgrounds by P1*kc*-mediated transduction according to (24).

PAGE and immunoblotting. Aliquots of 25 to 50 μg of protein from the indicated subcellular fractions were separated by sodium dodecyl sulfate-polyacrylamide gel electrophoresis (SDS-PAGE) using either 10% (wt/vol), 12.5% (wt/vol), or 15% (wt/vol) polyacrylamide gels (27) and transferred to nitrocellulose membranes as described previously (28). Antibodies raised against PflB (1:3,000) (4), a FocA peptide (1:500) (3), or purified FocA (1:3,000) were used. Secondary antibody conjugated to horseradish peroxidase was obtained from Bio-Rad. Visualization was done by the enhanced chemiluminescent reaction (Stratagene). The N-terminally Strep-tagged FocA fusion protein was purified as described previously (3) and used to raise polyclonal antibodies in rabbits according to the procedures of the company Seqlab (Germany).

Other methods. Analysis of *E. coli* fermentation products and the hypophosphite inhibition test were performed exactly as described previously (4). Determination of β-galactosidase enzyme activity was performed according to the method of Miller (24). S1 nuclease protection analysis of the *focA-pflB* transcripts was performed exactly as described previously (16). Protein concentration was determined according to the method of Lowry et al. (29). Densitometric analysis of the Western blots was performed using the ImageJ software from the National Institutes of Health (http:rsb.info.nih.gov/ij).

RESULTS

Correlation between the efficiency of *focA* translation and transcription of *pflB*. The translation initiation codon of the *focA* transcript is GUG (4). In a previous study with *lacZ* protein fusions it was shown that whereas conversion of the GUG codon to UUU or GUC prevented *focA* mRNA translation, conversion to an AUG codon increased expression ~10-fold (4). These changes in the *focA* translation initiation codon also affected the expression of a *focA-pflB-lacZ* protein fusion significantly due to polarity effects: prevention of *focA* translation decreased *pfl* expression 20- to 30-fold, while improved efficiency of *focA* translation initiation led to an ~3-fold increase in *pfl-lacZ* expression. To examine the consequences of these changes on transcription of the *focA-pflB* operon, total RNA was isolated from a set of strains harboring chromosomal mutations in the GUG codon of the *focA* gene. The strains were grown aerobically and anaerobically in rich medium and the isolated RNA was analyzed by S1 nuclease mapping of the *focA-pflB* transcripts, performed as previously described (12, 16). As a control, the transcript pattern of wild-type strain MC4100 was compared to that of the FocA$^-$ mutant REK701, which has two consecutive stop codons within the *focA* gene (see Table 1) but has an unaltered GUG translation initiation codon (4). Both strains exhibited similar transcript profiles (Fig. 1B), showing a clear anaerobic induction of transcription. The only differences in the transcript patterns were an additional transcript that was detected approximately halfway between transcripts 5 and 6+6a in REK701, possibly the result of a new processing site, and the intensity of both transcripts 5 and 6 was clearly less in the *focA* mutant compared to the wild-type strain. On the other hand, transcripts 1 through 4 were of a similar intensity to the wild type (Fig. 1B).

This transcript profile contrasts markedly with that observed for the *focA* mutants REK700 (GUG converted to UUU) and

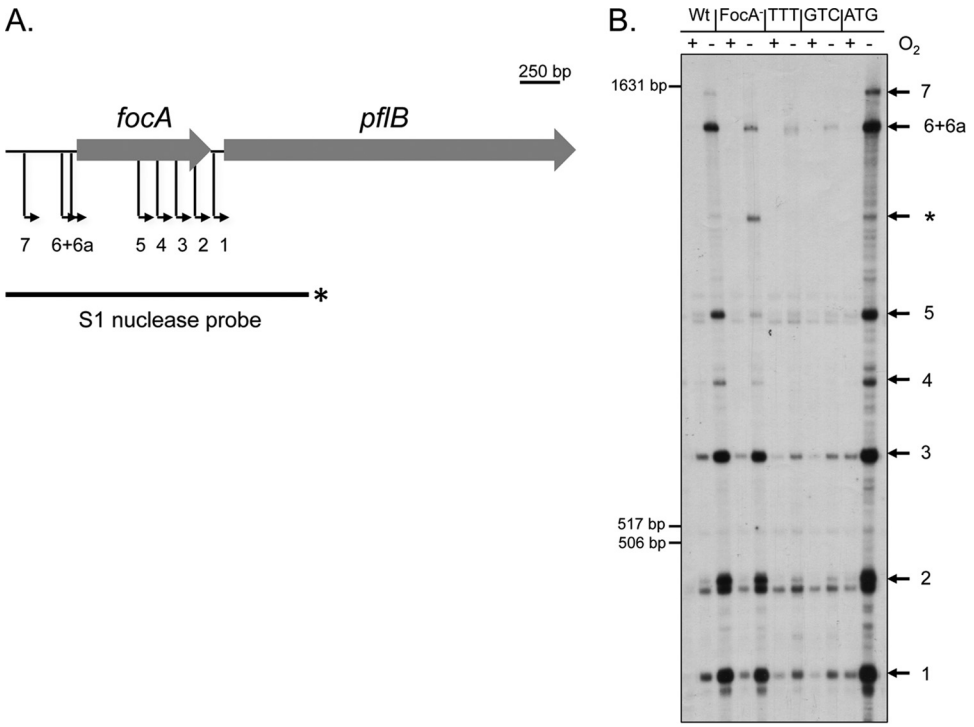

FIG 1 Transcriptional polarity within the *focA-pflB* operon caused by alterations in the *focA* translational initiation codon. (A) Schematic representation of the *focA-pflB* operon. The angled arrows labeled 1 through 7 represent the locations of the 5′ ends of transcripts. The ^{32}P-labeled DNA probe used for the S1 nuclease mapping experiment shown in panel B is depicted below the operon, and the asterisk indicates the labeled end. (B) Autoradiogram of a S1 nuclease protection assay of total RNA (50 μg) isolated from strains grown aerobically (+) or anaerobically (−) and hybridized with the single-stranded, labeled *focA-pflB′* DNA probe shown in panel A. The samples were separated on a denaturing polyacrylamide gel (4% [wt/vol]) and, after drying, the gel was exposed to X-ray film as described previously (12). The total RNA was isolated from the following strains: MC4100 (Wt), REK701 (FocA$^-$), REK700 (TTT), REK703 (GTC), and REK702 (ATG). The locations of the respective 5′ ends of the *focA-pflB* transcripts depicted in panel A are shown in the right of the panel, while the migration positions of DNA size markers are indicated on the left of the panel.

REK703 (GUG converted to GUC), where translation of the *focA* transcript was prevented (Fig. 1B, lanes 5 through 8). In both mutants each transcript was reduced in intensity when RNA was isolated from anaerobically grown cells, and the intensity levels were comparable to that of the wild type after growth with oxygen, i.e., the uninduced level. This finding agrees well with previously reported effects of the mutations on *pfl-lacZ* expression levels (4). Because conversion of the GUG codon to either UUU or GUC resulted in essentially identical transcript patterns, this indicates that the strong polar effect on downstream transcript levels was probably due to prevention of *focA* mRNA translation, resulting in more rapid transcript turnover (4), and not to direct transcriptional regulation. To confirm this hypothesis, we analyzed total RNA isolated from aerobically and anaerobically grown REK702 in which the GUG codon was converted to the more efficiently translated AUG codon. The results clearly show that, while the intensity of transcripts under aerobic conditions was similar to that in MC4100, the levels of transcripts after anaerobic growth were significantly increased (Fig. 1B, lanes 9 and 10). This was particularly apparent for transcripts 6+6a and 7, which are the transcripts that are translated to generate FocA. Together, these results show that mutations affecting the translation initiation efficiency of *focA* strongly influence the levels of the processed *focA-pflB* operon transcripts, which are ultimately translated to generate PflB.

To demonstrate the consequences of these mutations on the amounts of FocA and PflB in anaerobically growing *E. coli* cells, we performed Western blot experiments with either purified membrane fractions to analyze FocA (3) or soluble fractions to assess the levels of PflB (21) (Fig. 2). FocA is a low-abundance membrane protein in MC4100 and is only observed under anaerobic conditions (3, 4, 13). Antibodies raised against full-length FocA identified a weak band in MC4100 that migrated at its characteristic aberrant molecular mass of 22 kD (3, 4, 7) and which was absent in membranes isolated from strain REK701 (Fig. 2A). Conversion of the GUG translation initiation codon of the *focA* gene to AUG resulted in an ~20-fold increase in FocA levels in the membrane fraction, as determined by densitometric scanning of the autoradiogram. No FocA protein could be detected in the membrane fractions of either strain REK700 (GUG to UUU) or REK703 (GUG to GUC), a finding consistent with the lack of translation of the *focA* mRNA (Fig. 2B). It was noted that FocA synthesis was significantly increased in strain RM220, which has a deletion in the genes encoding PflB and its activating enzyme PflA (21), compared to wild-type strain MC4100. Densitometric analysis of the blot revealed that the level of FocA in RM220 was ~5-fold lower than in REK702 (GUG to AUG). This result is consistent with the findings of previous transcriptional studies in which it was shown that increased levels of pyruvate in the cell cause increased expression of the *focA-pflB* operon, as well as enhanced levels of PflB protein (11, 15).

To examine the consequences of the *focA* start codon muta-

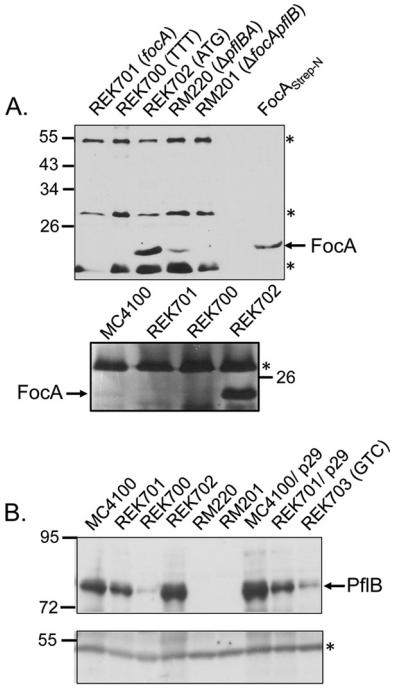

FIG 2 Influence of various *focA* mutations on anaerobic FocA and PflB synthesis. Membrane fractions (50 μg of protein) or soluble fractions (30 μg of protein) prepared from the indicated strains were separated on 15% (wt/vol) or 10% (wt/vol) SDS-polyacrylamide gels, respectively. After transfer to a nitrocellulose membrane, the filters were probed with antiserum raised against *E. coli* FocA peptide (amino acids 141 to 159 [3]) (upper part of panel A), FocA (lower part of panel A) or PflB (B). In the lower part of panel A, the samples were run on a 15% (wt/vol) polyacrylamide gel, and the autoradiogram was exposed for twice the length of time compared to others to visualize FocA in MC4100 (identified by the arrow). The strains used to generate the subcellular fractions are indicated above the respective lanes. Purified, N-terminally Strep-tagged FocA (80 ng) was used as control in panel A. Plasmid p29 carries the complete *focA-pflB* operon on a multicopy plasmid. The migration positions of molecular mass markers are indicated on the left, and the migration positions of FocA or PflB are indicated on the right of the figure. The asterisks denote unidentified cross-reacting polypeptides that acted as loading controls in each experiment.

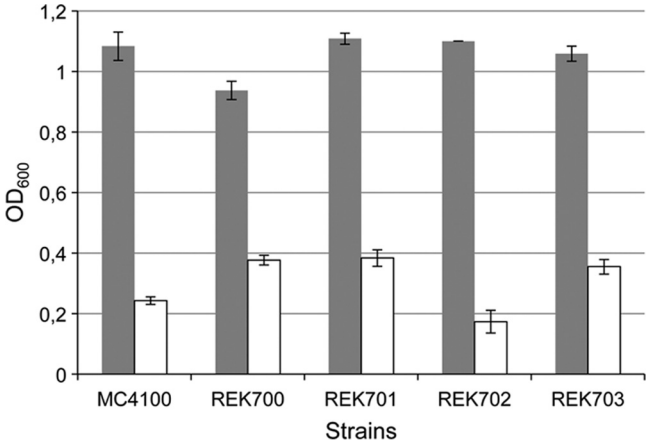

FIG 3 Increased FocA synthesis results in enhanced sensitivity of strains to hypophosphite. The indicated strains were grown anaerobically for 24 h at 37°C in WM-medium (pH 6.8) with glucose as the carbon source, either in the absence (gray bars) or presence (white bars) of 75 mM sodium hypophosphite. The ODs of three independent cultures were determined. The growth rate of MC4100 in the presence of 75 mM hypophosphite was 0.115 h^{-1}, and that of REK702 was 0.069 h^{-1}. Both had a comparable growth rate of 0.34 h^{-1} in the absence of hypophosphite.

tions on PflB levels, we analyzed soluble fractions of each strain by immunoblotting with antibodies raised against PflB (21). A soluble fraction derived from the *focA* mutant REK701 had levels of PflB similar to those observed in MC4100 (wild type) after anaerobic growth of cells (Fig. 2B). This result is consistent with previous findings (4) and indicates that as long as translation of the *focA* gene can be initiated, there is a limited polar effect on PflB synthesis, despite the absence of a FocA protein due to the introduction of consecutive stop codons after codon 113 in *focA* (see Table 1). This contrasts strongly with the situation when *focA* translation was impeded by mutation of the GUG codon to UUU (strain REK700) or GUC (strain REK703), where extracts revealed an ~10-fold reduction in PflB levels compared to the wild type (Fig. 2B). The negative controls RM220 and RM201, both of which carry deletions in the *pflB* gene (11, 21), completely lacked PflB antigen. Conversion of the GUG codon to AUG in *focA* (strain REK702) resulted in a 2- to 3-fold increase in PflB levels (Fig. 2B). This level was similar to that observed when the low-copy-number plasmid p29 (30) carrying the complete *focA-pflB* operon was introduced into MC4100. This suggests that PflB levels cannot be overproduced above a certain level when *pflB* is coexpressed with *focA*.

Sensitivity toward hypophosphite correlates directly with FocA levels. In a previous study, insertion mutations in the *focA* gene were identified based on an enhanced resistance to the formate analogue hypophosphite (4). Therefore, we used this assay to test whether the conversion of the GUG to an AUG codon resulted in enhanced sensitivity to hypophosphite. REK702 (GUG to AUG) was grown in minimal glucose medium containing 75 mM hypophosphite, and the optical density of the anaerobic culture was monitored at 600 nm (OD_{600}) after 24 h of incubation at 37°C (Fig. 3). Although REK702 showed growth similar to that of the wild-type MC4100 in the absence of hypophosphite, it showed poorer growth in the presence of hypophosphite compared to MC4100. In contrast, strains REK700 (GUG to UUU), REK701 (Stop), and REK703 (GUG to GUC) showed better growth than the wild type, which is consistent with the lack of FocA (Fig. 3). These findings indicate that overproduction of FocA results in enhanced sensitivity to hypophosphite.

FocA is not limiting for formate translocation across the cytoplasmic membrane in *E. coli* during fermentation. To examine the consequences of increasing FocA levels on formate export and reimport by fermenting *E. coli* cells, we examined over a 14-h period the fermentation product spectrum of formate, pyruvate, lactate, succinate, and acetate during anaerobic growth in minimal medium with glucose as a carbon source. Growth, as well as the pH of the culture medium, was also monitored (Fig. 4). Formate started to accumulate in the medium of MC4100 cultures as soon as growth initiated, reaching a maximum of 9 mM OD_{420}^{-1} after 4 h (Fig. 4A), which equated to approximately mid-exponential phase of growth (Fig. 4B). Thereafter, formate levels in the culture medium steadily decreased, and by 10 h all of the formate had been reimported into the cells (Fig. 4A). The initiation of formate uptake roughly correlated with the decrease in the pH of the culture, which finally stabilized at pH 6.2 after 14 h (Fig. 4B). Of the five fermentation products monitored throughout growth,

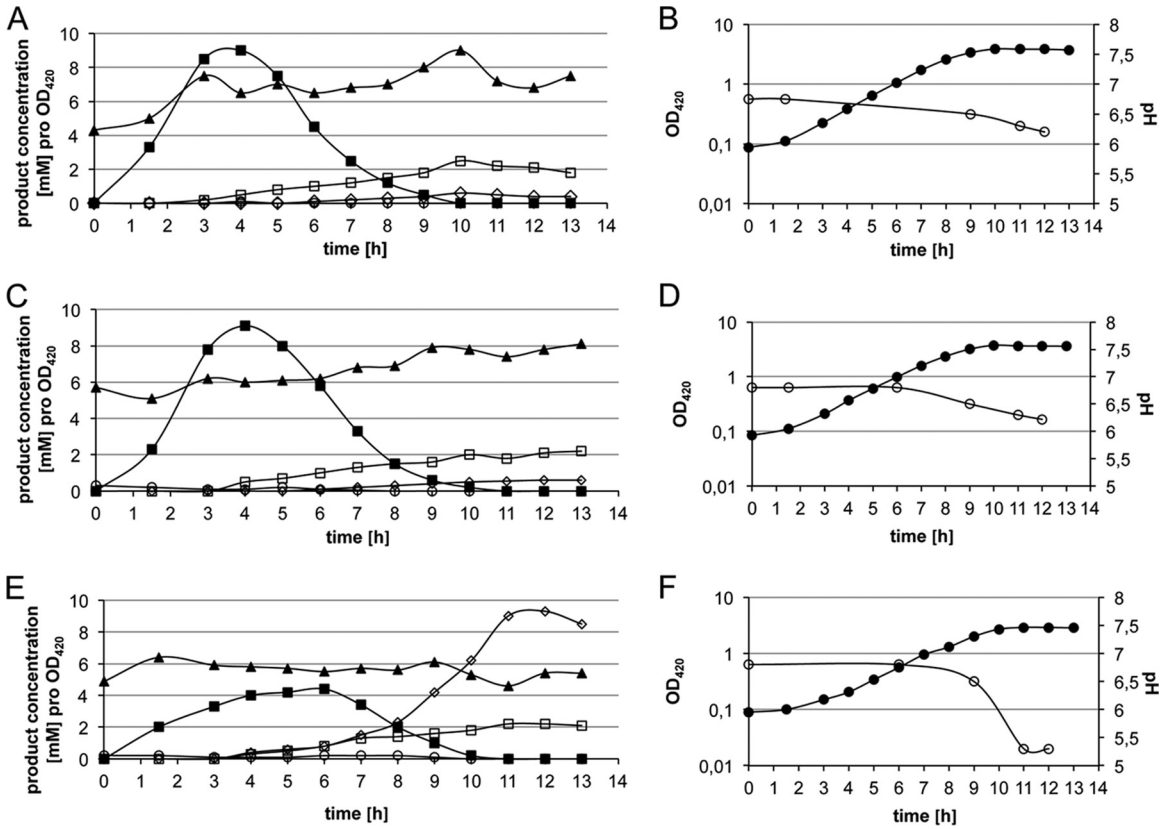

FIG 4 Fermentation product spectra of *focA* translation initiation codon mutants. MC4100 (A and B), REK702 (C and D), and REK703 (E and F) were cultured in WM-medium (pH 6.8) with glucose as carbon source, and the organic acids were extracted from the culture medium at the time points indicated and quantified by high-pressure liquid chromatography analysis (4). In panels A, C, and E the symbols are defined as follows: ■, formate; □, succinate; ▲, acetate; ○, pyruvate; and ◇, lactate. The concentration of each metabolite was calculated with respect to the OD of the culture. Panels B, D, and F show the corresponding growth curves of the strains and the pH of the culture medium during growth.

only formate was reimported from the culture medium. Acetate levels steadily increased from 5 to 8 mM OD_{420}^{-1}, while succinate also slowly attained levels of 1 mM OD_{420}^{-1}. In contrast, pyruvate and lactate remained at a low, barely detectable level (Fig. 4A).

Surprisingly, the fermentation product profile of strain REK702 was almost indistinguishable from that of MC4100 (Fig. 4C). Moreover, the growth curve and pH profile were also essentially superimposable (Fig. 4D). This result indicates that FocA is not limiting in wild-type *E. coli* cells with respect to formate translocation. Moreover, despite the increase in PflB levels in REK702, this had no influence on formate production, indicating that PflB levels are also not growth limiting in fermenting *E. coli* cells.

The absence of FocA had a marked effect on the fermentation product profile of strain REK703 (GUG to GUC). First, approximately only half the amount of formate was secreted into the culture medium compared to MC4100 (Fig. 4E). Nevertheless, despite the fact that REK703 showed an ~10-fold-reduced level of PflB (see Fig. 2B), it still produced significant amounts of formate. Earlier studies demonstrated that *E. coli* has a second, as-yet-unidentified, system for exporting formate (30). The high levels of lactate production from mid-exponential growth phase continuing into the stationary growth phase indicate, however, that all of the pyruvate derived from glucose could not be metabolized by PflB, and the excess was reduced and exported as lactate. This correlates also with the lower pH of 5.4 in the growth medium of REK703 (Fig. 4F). Notably, the profiles of both acetate and succinate remained similar to those of MC4100 (Fig. 4E). The fermentation product profile of strain REK700 (GUG to UUU) was indistinguishable from that of strain REK703 (data not shown).

The inability to metabolize formate hinders the import of extracellular formate. A mutant lacking any of the *sel* gene products fails to synthesize the selenocysteine-containing FDHs (31, 32). In order to assess whether the ability of the strain to metabolize formate affected formate export or import, we examined the fermentation product profile of a *selC* mutant after growth in glucose minimal medium (Fig. 5A). Formate was secreted into the culture medium at a similar stage of growth as seen for wild type. Despite the presence of FocA, however, formate was not reimported and it accumulated in the culture medium to levels nearing 20 mM OD_{420}^{-1}. Although the acetate and succinate profiles of strain FM460 were similar to those of MC4100, lactate was exported during the late exponential phase of growth, accumulating to 10 mM OD_{420}^{-1} (Fig. 5A). This caused the pH of the culture medium to decrease to 5.5 in the late exponential phase growth (Fig. 5B). Otherwise, the growth curve was similar to that of MC4100.

To ensure that the observed lack of formate import by strain FM460 was solely due to the lack of FDHs and not caused by a secondary consequence of the *selC* mutation, we analyzed the fer-

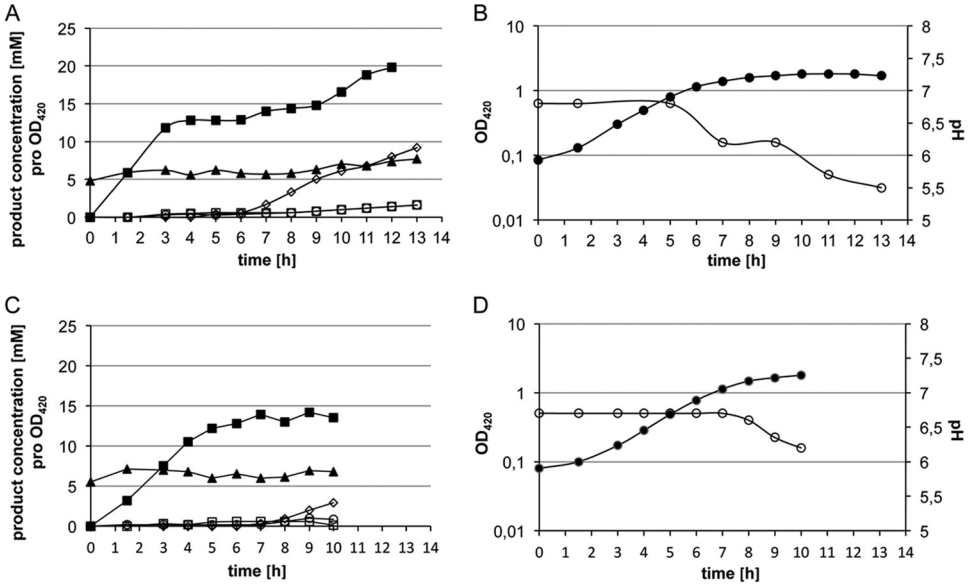

FIG 5 Defects in FDH synthesis prevent reimport of formate. FM460 (*selC*) (A and B) and WL308 (FDH$^-$) (C and D) were cultured in WM-medium (pH 6.8) with glucose as carbon source, and the organic acids (A and C) and the growth and pH (B and D) were analyzed as described in the legend to Fig. 4. In panels A and C, the symbols are defined as follows: ■, formate; □, succinate; ▲, acetate; ○, pyruvate; and ◇, lactate.

mentation product spectrum of strain WL308, which lacks the *fdhD* and *fdhE* genes and thus cannot synthesize active FDHs (20, 22, 33). Like the *selC* mutant, strain WL308 failed to reimport formate (Fig. 5C), whereas acetate and succinate levels remained similar to those of the wild type. The level of formate exported was marginally lower than that exported by FM460; however, this might be due to the poorer growth exhibited by WL308 (Fig. 5D). The reason for the poorer growth under these conditions is currently unclear.

DISCUSSION

The recent important discovery that purified FocA in reconstituted planar lipid bilayers translocates not only formate but also other monovalent anionic products of mixed-acid fermentation such as acetate, lactate, and pyruvate (10) led to the suggestion that FocA might perform the same function *in vivo*. The findings of the present study suggest, however, that whereas formate is both exported and reimported by FocA in fermenting *E. coli* cells, lactate, acetate, and succinate export did not show the same correlation with FocA *in vivo*. Moreover, succinate, acetate, and lactate steadily accumulated in the medium, suggesting that they were not taken up by *E. coli* cells under the conditions analyzed. Increasing the levels of FocA in anaerobic cells or prevention of FocA synthesis had no effect on the levels or kinetics of export of either acetate or succinate in comparison to the wild type. Indeed, lactate export was increased in *focA* mutants, presumably because pyruvate was reduced by lactate dehydrogenase, even though PflB was present. Taken together, these data suggest that FocA is a formate-specific channel *in vivo*. These findings raise the question as to how selectivity toward formate is achieved *in vivo*. One possibility is that there is pH-dependent gating of the FocA channel, as has been previously suggested (6, 7). However, this would presumably have to be highly localized to account for the fact that the cytoplasmic pH is generally maintained near neutrality. An alternative possibility is that the substrate selectivity of FocA is determined by an interaction partner. Studies to determine whether either of these possibilities can explain formate selectivity are currently being undertaken.

The chloride, nitrite, and hypophosphite anions were also shown recently to be translocated through FocA *in vitro* (9). Although no conclusions regarding nitrite and chloride translocation by FocA *in vivo* could be drawn from the present study, it was clearly shown that conversion of the GUG translation initiation codon to the more efficient AUG resulted in enhanced sensitivity of REK702 to sodium hypophosphite, whereas mutants lacking FocA were more resistant to hypophosphite compared to either REK702 or MC4100 (wild type). This confirms a previous observation (4) that FocA is effective at taking up hypophosphite. With a pK_a of 1.1 hypophosphite is essentially always present as the anion at neutral pH and therefore requires transport into *E. coli* cells. Clearly, FocA is one of the main routes by which hypophosphite enters cells. The increased hypophosphite sensitivity of REK702 correlated well with the increased amount of FocA in the cell compared to the wild type. Through the use of specific antibodies, we could show that FocA levels were increased ~20-fold when the GUG codon was converted to AUG on the chromosome, an observation that agrees reasonably well with the results of previous *focA-lacZ* fusion studies (4). Notably, despite the increased level of FocA in strain REK702, the amount of formate exported by the strain remained unaffected, indicating that the roughly 100 FocA pentamers calculated to be present in anaerobically growing *E. coli* cells (3) was not limiting with regard to either formate export or import. The increased levels of FocA apparently also had no significant effect on the levels of mixed-acid fermentation products generated by *E. coli*. Moreover, analysis of *focA-pflB* transcript levels, *pflB-lacZ* expression data (4), and immunological studies demonstrated that PflB levels were also increased ~3-fold in REK702. Despite this increase in PflB synthesis, no significant effect on the fermentative metabolism of the strain was apparent, which indicates that PflB is also not limiting in the an-

aerobic cell. In addition, the strong polar effect caused by prevention of *focA* translation, through mutation of the translation initiation codon to either UUU or GUC, on downstream *pflB* expression resulted in a 10- to 20-fold reduction in the intracellular levels of PflB. Nonetheless, formate was still synthesized, albeit in significantly reduced amounts compared to the wild type, which also agreed with reduced hydrogen production by REK700 and REK703 (B. Suppmann and R. G. Sawers, unpublished data). These data indicate that *E. coli* can adapt its metabolism to ensure glycolytic flux is maintained, even when the level of PflB varies considerably; however, this impacts on formate excretion and uptake.

Finally, the effect of preventing intracellular or periplasmic utilization of formate by blocking the selenocysteine biosynthesis pathway (20, 32) or preventing maturation of the FDHs demonstrated that formate, once exported, remained in the growth medium. Although perhaps not unexpected, this result is in accord with the function of a channel and provides *E. coli* with an elegant mechanism to allow substrate access to either side of the membrane: if an electron acceptor is present then formate can preferentially be oxidized by the energy-conserving, periplasmically oriented FDH-O or FDH-N enzymes (2, 18); if no acceptor is available, formate can be reimported and disproportionated to dihydrogen and carbon dioxide by the formate hydrogenlyase complex, thus offsetting acidification of the cytoplasm. Notably, the same result was observed for strains REK701 (stop codon within *focA*) and REK703 (GUG to GTC) when the *selC* allele was introduced (data not shown), which also suggests that the unidentified protein responsible for formate translocation in the absence of FocA exhibits channel-like activity. Construction of *focA nirC* double-null mutants have demonstrated that NirC is not responsible for residual formate translocation in *focA* mutants (L. Beyer, B. Suppmann, and R. G. Sawers, unpublished data). Because energy conservation is a premium during fermentation a channel-based translocation system tightly coupled to intracellular metabolism of formate, together with an acidic environment outside the cell, provides the driving force for formate import. This system is also poised perfectly by the corresponding K_m values of the FDHs and the formate-dependent transcriptional regulator FhlA for formate so that substrate is initially offered for respiration, and only once it accumulates is it reimported and disproportionated to CO_2 and H_2 by the formate hydrogenlyase complex (1, 34). Reimportation of formate initiates in the late exponential phase of growth and appears to show an inverse correlation with PflB activity (1, 2, 34).

The widespread occurrence of FNT channels with specificity for different monovalent anionic substrates, especially among anaerobes, suggests that these evolutionarily ancient membrane proteins might provide an effective means of energy-independent, pH-driven substrate translocation.

ACKNOWLEDGMENTS

This study was supported by the GRK1026 (Conformational Transitions in Macromolecular Interactions) from the Deutsche Forschungsgemeinschaft and by the Exzellenzinitiative of the region of Saxony-Anhalt.

REFERENCES

1. **Sawers G, Blokesch M, Böck A.** September 2004, posting date. Chapter 3.5.4, Anaerobic formate and hydrogen metabolism. *In* Böck A, Curtiss R, III, Kaper JB, Karp PD, Neidhardt FC, Nyström T, Slauch JM, Squires CL, Ussery D (ed), EcoSal–*Escherichia coli* and *Salmonella*: cellular and molecular biology. ASM Press, Washington, DC. doi:10.1128/ecosal.3.4.5.
2. **Sawers RG.** 2005. Formate and its role in hydrogen production in *Escherichia coli*. Biochem. Soc. Trans. **33**:42–46.
3. **Falke D, Schulz K, Doberenz C, Beyer L, Lilie H, Thiemer B, Sawers RG.** 2010. Unexpected oligomeric structure of the FocA formate channel of *Escherichia coli*: a paradigm for the formate-nitrite transporter family of integral membrane proteins. FEMS Microbiol. Lett. **303**:69–75.
4. **Suppmann B, Sawers G.** 1994. Isolation and characterisation of hypophosphite-resistant mutants of *Escherichia coli*: identification of the FocA protein, encoded by the *pfl* operon, as a putative formate transporter. Mol. Microbiol. **11**:965–982.
5. **Lü W, Du J, Wacker T, Gerbig-Smentek E, Andrade SL, Einsle O.** 2011. pH-dependent gating in a FocA formate channel. Science **332**:352–354.
6. **Waight AB, Love J, Wang DN.** 2010. Structure and mechanism of a pentameric formate channel. Nat. Struct. Mol. Biol. **17**:31–37.
7. **Wang Y, Huang Y, Wang J, Cheng C, Huang W, Lu P, Xu YN, Wang P, Yan N, Shi Y.** 2009. Structure of the formate transporter FocA reveals a pentameric aquaporin-like channel. Nature **462**:467–472.
8. **Czyzewski BK, Wang DN.** 2012. Identification and characterization of a bacterial hydrosulphide ion channel. Nature **483**:494–497.
9. **Lü W, Schwarzer NJ, Du J, Gerbig-Smentek E, Andrade SL, Einsle O.** 2012. Structural and functional characterization of the nitrite channel NirC from *Salmonella typhimurium*. Proc. Natl. Acad. Sci. U. S. A. **109**:18395–18400.
10. **Lü W, Du J, Schwarzer NJ, Gerbig-Smentek E, Einsle O, Andrade SL.** 2012. The formate channel FocA exports the products of mixed-acid fermentation. Proc. Natl. Acad. Sci. U. S. A. **109**:13254–13259.
11. **Sawers G, Böck A.** 1988. Anaerobic regulation of pyruvate formate-lyase from *Escherichia coli* K-12. J. Bacteriol. **170**:5330–5336.
12. **Sawers G, Böck A.** 1989. Novel transcriptional control of the pyruvate formate-lyase gene: upstream regulatory sequences and multiple promoters regulate anaerobic expression. J. Bacteriol. **171**:2485–2498.
13. **Sawers G.** 1993. Specific transcriptional requirements for positive regulation of the anaerobically inducible *pfl* operon by ArcA and FNR. Mol. Microbiol. **10**:737–747.
14. **Sawers G, Suppmann B.** 1992. Anaerobic induction of pyruvate formate-lyase gene expression is mediated by the ArcA and FNR proteins. J. Bacteriol. **174**:3474–3478.
15. **Sirko A, Zehelein E, Freundlich M, Sawers G.** 1993. Integration host factor is required for anaerobic pyruvate induction of *pfl* operon expression in *Escherichia coli*. J. Bacteriol. **175**:5769–5777.
16. **Sawers RG.** 2005. Evidence for novel processing of the anaerobically inducible dicistronic *focA-pfl* mRNA transcript in *Escherichia coli*. Mol. Microbiol. **58**:1441–1453.
17. **Sawers RG.** 2006. Differential turnover of the multiple processed transcripts of the *Escherichia coli focA-pflB* operon. Microbiology **152**:2197–2205.
18. **Sawers RG.** 1994. The hydrogenases and formate dehydrogenases of *Escherichia coli*. Antonie Van Leeuwenhoek **66**:57–88.
19. **Casadaban MJ.** 1976. Transposition and fusion of the *lac* genes to selected promoters in *Escherichia coli* using bacteriophage lambda and Mu. J. Mol. Biol. **104**:541–555.
20. **Sawers G, Heider J, Böck A.** 1991. Expression and operon structure of the *sel* genes of *Escherichia coli* and identification of a third selenium-containing formate dehydrogenase isoenzyme. J. Bacteriol. **173**:4983–4993.
21. **Heßlinger C, Fairhurst SA, Sawers G.** 1998. Novel keto acid formate-lyase and propionate kinase enzymes are components of an anaerobic pathway in *Escherichia coli* that degrades L-threonine to propionate. Mol. Microbiol. **27**:477–492.
22. **Heider J, Böck A.** 1992. Targeted insertion of selenocysteine into the α subunit of formate dehydrogenase from *Methanobacterium formicicum*. J. Bacteriol. **174**:659–663.
23. **Begg Y, Whyte J, Haddock B.** 1977. The identification of mutants of *Escherichia coli* deficient in formate dehydrogenase and nitrate reductase activities using dye indicator plates. FEMS Microbiol. Lett. **2**:47–50.
24. **Miller J.** 1972. Experiments in molecular genetics. Cold Spring Harbor Laboratory, Cold Spring Harbor, NY.
25. **Fraenkel DA, Neidhardt FC.** 1961. Use of chloramphenicol to study control of RNA synthesis in bacteria. Biochim. Biophys. Acta **53**:96–100.
26. **Hormann K, Andreesen J.** 1989. Reductive cleavage of sarcosine and

betaine by *Eubacterium acidaminophilum* via enzyme systems different from glycine reductase. Arch. Microbiol. **153**:50–59.
27. **Laemmli U.** 1970. Cleavage of structural proteins during the assembly of the head of bacteriophage T4. Nature **227**:680–685.
28. **Towbin H, Staehelin T, Gordon J.** 1979. Electrophoretic transfer of proteins from polyacrylamide gels to nitrocellulose sheets: procedure and some applications. Proc. Natl. Acad. Sci. U. S. A. **76**:4350–4354.
29. **Lowry O, Rosebrough N, Farr A, Randall R.** 1951. Protein measurement with the Folin phenol reagent. J. Biol. Chem. **193**:265–275.
30. **Christiansen L, Pedersen S.** 1981. Cloning, restriction endonuclease mapping and posttranscriptional regulation of *rpsA*, the structural gene for ribosomal protein S1. Mol. Gen. Genet. **181**:548–551.
31. **Leinfelder W, Forchhammer K, Zinoni F, Sawers G, Mandrand-Berthelot M, Böck A.** 1988. *Escherichia coli* genes whose products are involved in selenium metabolism. J. Bacteriol. **170**:540–546.
32. **Zinoni F, Birkmann A, Stadtman T, Böck A.** 1986. Nucleotide sequence and expression of the selenocysteine-containing polypeptide of formate dehydrogenase (formate-hydrogenlyase-linked) from *Escherichia coli*. Proc. Natl. Acad. Sci. U. S. A. **83**:4650–4654.
33. **Schlindwein C, Giordano G, Santini CL, Mandrand MA.** 1990. Identification and expression of the *Escherichia coli fdhD* and *fdhE* genes, which are involved in the formation of respiratory formate dehydrogenase. J. Bacteriol. **172**:6112–6121.
34. **Rossmann R, Sawers G, Böck A.** 1991. Mechanism of regulation of the formate-hydrogenlyase pathway by oxygen, nitrate, and pH: definition of the formate regulon. Mol. Microbiol. **5**:2807–2814.